

Uranium(IV) Alkyl Complexes of a Rigid Dianionic NON-Donor Ligand: Synthesis and Quantitative Alkyl Exchange Reactions with Alkylolithium Reagents

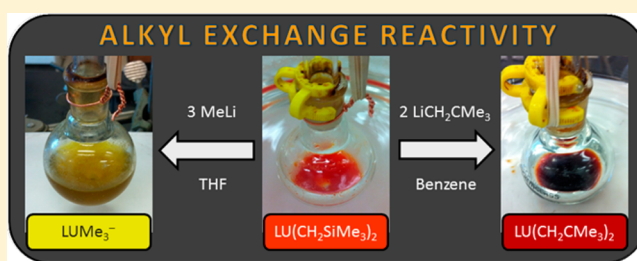
Nicholas R. Andreychuk,[†] Sougandi Ilango,[†] Balamurugan Vidjayacoumar,[†] David J. H. Emslie,^{*,†} and Hilary A. Jenkins[‡]

[†]Department of Chemistry and Chemical Biology, McMaster University, 1280 Main Street West, Hamilton, Ontario L8S 4M1, Canada

[‡]McMaster University Analytical X-ray Diffraction Facility, McMaster University, 1280 Main Street West, Hamilton, Ontario L8S 4M1, Canada

S Supporting Information

ABSTRACT: Reaction of $[(\text{XA}_2)\text{UCl}_3\{\text{K}(\text{dme})_3\}]$ ($\text{XA}_2 = 4,5\text{-bis}(2,6\text{-diisopropylanilino})\text{-}2,7\text{-di-}t\text{-tert-butyl-}9,9\text{-dimethyl-xanthene}$) with 2 equiv of ((trimethylsilyl)methyl)lithium or neopentylolithium afforded red-orange $[(\text{XA}_2)\text{U}(\text{CH}_2\text{SiMe}_3)_2]$ (**1**) and dark red $[(\text{XA}_2)\text{U}(\text{CH}_2\text{CMe}_3)_2]$ (**2**), respectively. Reaction of **1** with an additional 1 equiv of $\text{LiCH}_2\text{SiMe}_3$ in THF yielded yellow $[\text{Li}(\text{THF})_x][(\text{XA}_2)\text{U}(\text{CH}_2\text{SiMe}_3)_3]$ (**3**), and reaction of $[(\text{XA}_2)\text{UCl}_3\{\text{K}(\text{dme})_3\}]$ with 3 equiv of methylolithium in dme afforded yellow $[\text{Li}(\text{dme})_3][(\text{XA}_2)\text{-U}(\text{Me})_3]$ (**4**). Reaction of **1** with 2.1 equiv of $\text{LiCH}_2\text{CMe}_3$ in benzene resulted in rapid conversion to **2**, with release of 2 equiv of $\text{LiCH}_2\text{SiMe}_3$. Similarly, reaction of **1** with 3.3 equiv of MeLi in THF provided **4** as the $[\text{Li}(\text{THF})_x]^+$ salt, accompanied by 2 equiv of $\text{LiCH}_2\text{SiMe}_3$. These unusual alkyl exchange reactions resemble salt metathesis reactions, but with elimination of an alkylolithium instead of a lithium halide. Addition of a large excess of $\text{LiCH}_2\text{SiMe}_3$ to **2** or **4** did not generate detectable amounts of **1** by NMR spectroscopy, suggesting that the equilibrium in these reactions lies far to the side of complexes **2** and **4**. In contrast, the reaction of $[(\text{XA}_2)\text{Th}(\text{CH}_2\text{SiMe}_3)_2]$ (**1-Th**) with 2.2 equiv of $\text{LiCH}_2\text{CMe}_3$ yielded an approximate 1:1:3:1 mixture of $[(\text{XA}_2)\text{Th}(\text{CH}_2\text{CMe}_3)_2]$ (**2-Th**), $[(\text{XA}_2)\text{Th}(\text{CH}_2\text{SiMe}_3)(\text{CH}_2\text{CMe}_3)]$ (**5-Th**), $\text{LiCH}_2\text{SiMe}_3$, and $\text{LiCH}_2\text{CMe}_3$.



INTRODUCTION

The early actinide elements occupy a unique position in the periodic table where the f orbitals have sufficient radial extension to interact with the ligands and can play an important role in bonding. Additionally, uranium is able to gain ready access to a significantly non-lanthanide-like range of oxidation states, from III to VI.¹ These attributes have the potential to lead to organometallic reactivity inaccessible with transition-metal and lanthanide complexes, ideally resulting in new and productive applications for depleted uranium,² a byproduct of nuclear isotope enrichment that is currently stockpiled in large quantities. However, the organometallic chemistry of the actinide elements, relative to that of the transition metals and lanthanides, has been slow to develop, despite very early research efforts to prepare homoleptic actinide alkyl complexes^{3–7} during the Manhattan project.^{7,8} Consequently, the behavior of actinide organometallic complexes in fields such as olefin polymerization, olefin hydroelementation, small-molecule (e.g., carbon dioxide) activation, chemical vapor deposition (CVD), and atomic layer deposition (ALD) remains comparatively unexplored. Furthermore, the majority of actinide alkyl chemistry has involved carbocyclic ligand

complexes, in particular cyclopentadienyl and cyclooctatetraenyl complexes.⁸ In contrast, actinide alkyl complexes supported by multidentate noncarbocyclic ligand anions are scarce (Figure 1), despite the potential for such ligands to provide access to complexes with unique and readily tunable steric and electronic properties.

We have previously employed McConville's BDPP ligand and our own XA_2 ligand for the synthesis of neutral thorium(IV) bis((trimethylsilyl)methyl) and dibenzyl complexes, and these complexes were shown to exhibit high thermal stability, comparable to that of bis-(pentamethylcyclopentadienyl) analogues.^{3,16,19} Reaction of the neutral thorium dialkyls with $\text{B}(\text{C}_6\text{F}_5)_3$ and $[\text{CPh}_3][\text{B}(\text{C}_6\text{F}_5)_4]$ provided access to the first non-cyclopentadienyl thorium alkyl cations, for example $[(\text{XA}_2)\text{Th}(\text{CH}_2\text{SiMe}_3)(\eta^6\text{-benzene})][\text{B}(\text{C}_6\text{F}_5)_4]$, and a rare example of a thorium dication, $[(\text{XA}_2)\text{Th}\{\eta^6\text{-PhCH}_2\text{B}(\text{C}_6\text{F}_5)_3\}_2]$.^{17,19} We recently also pre-

Special Issue: Recent Advances in Organo-f-Element Chemistry

Received: November 24, 2012

Published: February 19, 2013

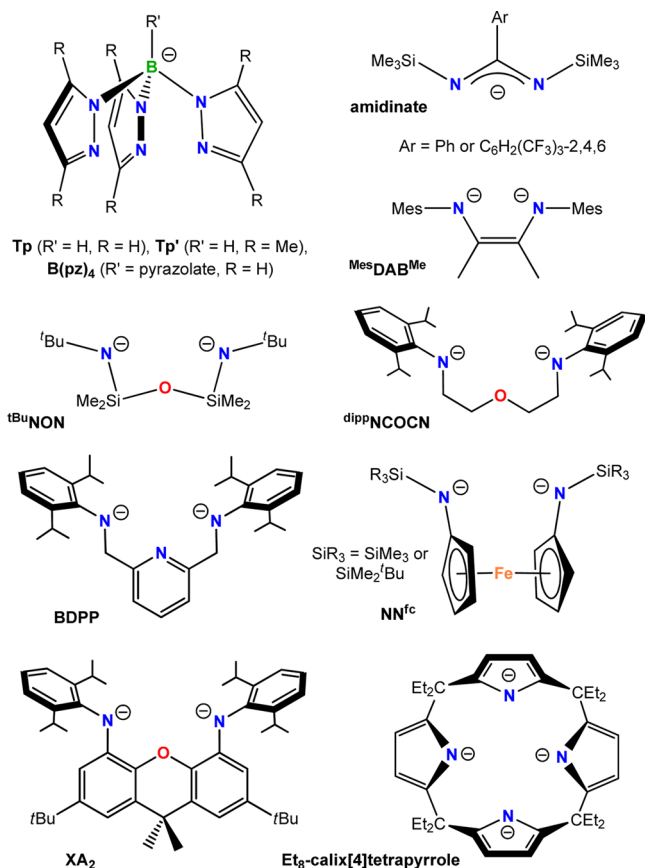


Figure 1. Multidentate anionic ligands previously employed in the synthesis of actinide alkyl⁹ complexes: (a) Tp,¹⁰ Tp',¹¹ and B(pz)₄ (pz = pyrazolate);¹² (b) amidinate;¹³ (c) MesDABMe;⁶ (d) tBuNON;^{14,15} (e) dippNCOCN;¹⁵ (f) BDPP;^{3,5,16,17} (g) NN^{fc};^{5,18} (h) XA₂;^{3,17,19} (i) Et₈-calix[4]tetrapyrrole.²⁰

pared an NSN-donor analogue of the XA₂ ligand, TXA₂, and reported a study of U–O versus U–S covalency in tri- and tetravalent uranium XA₂ and TXA₂ chloro complexes.²¹ Herein we describe the synthesis of neutral uranium(IV) dialkyl and anionic uranium(IV) trialkyl complexes prepared either from [(XA₂)UCl₃{K(dme)₃}] by salt metathesis or from [(XA₂)U-

(CH₂SiMe₃)₂] (**1**) via unusual alkyl exchange reactivity. For the purpose of comparison, the alkyl exchange reaction between [(XA₂)Th(CH₂SiMe₃)₂] (**1-Th**) and LiCH₂CMe₃ was also investigated.

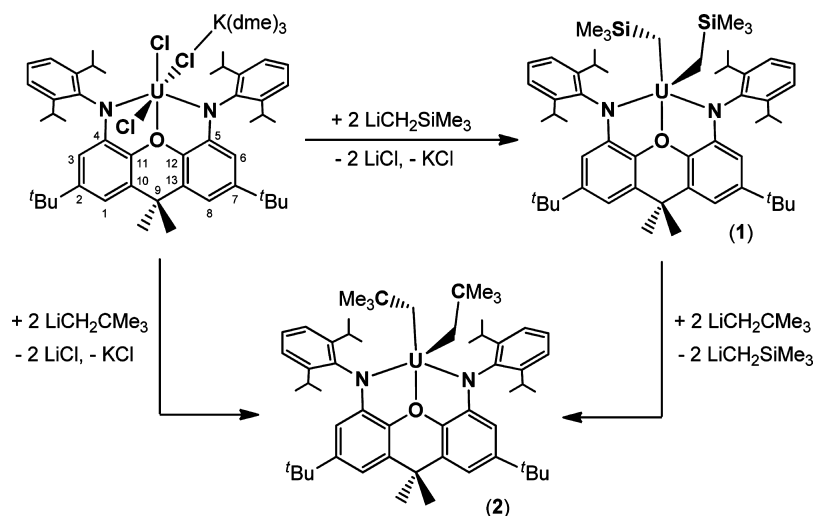
RESULTS AND DISCUSSION

Reaction of [(XA₂)UCl₃{K(dme)₃}] with 2 equiv of LiCH₂SiMe₃ afforded highly soluble [(XA₂)U(CH₂SiMe₃)₂] (**1**; Scheme 1), which was obtained as red-orange crystals in 64% yield after crystallization from hexanes at −30 °C. The room-temperature ¹H NMR spectrum of **1** in C₆D₆ or toluene-*d*₈ (Figure 2) shows only four signals: those for the *tert*-butyl groups, the para positions of the 2,6-diisopropylphenyl rings, and the CH^{1,8} and CH^{3,6} positions of the xanthene backbone. These signals are unaffected by the top–bottom symmetry of the molecule, since they lie in the plane of the xanthene backbone of the ligand. All other signals are broadened into the baseline due to a fluxional process which exchanges the axial and in-plane CH₂SiMe₃ groups. However, at low temperature, a full complement of ¹H NMR signals was observed, ranging from +180 to −225 ppm at −60 °C (Figure 2), indicative of C_s symmetry.

The X-ray crystal structure of **1**·2(*n*-hexane) (Figure 3 and Table 1) has two independent but structurally analogous five-coordinate molecules in the unit cell, each with one CH₂SiMe₃ group in an axial position and one located approximately in the plane of the ancillary ligand backbone. The four anionic donors (we are not suggesting that **1** is four-coordinate) adopt a distorted-tetrahedral arrangement with N–U–N, C–U–C, and N–U–C angles of 123.7(2)–123.9(2), 102.7(3)–105.4(3), and 101.1(2)–112.0(3)°, respectively. The neutral oxygen donor is located 0.92 and 0.95 Å out of the NUN plane in the direction of the axial alkyl group, and the complex has approximate C_s symmetry, consistent with the low-temperature ¹H NMR spectra.

The U–C distances of 2.368(7)–2.418(7) Å are comparable with those observed for the other crystallographically characterized neutral uranium(IV) (trimethylsilyl)methyl complex, Leznoff's [(O(CH₂CH₂NAr)₂U(CH₂SiMe₃)₂] (Ar = 2,6-diisopropylphenyl; U–C = 2.40(2) and 2.44(2) Å), but are shorter than those in Hayton's anionic [Li₄(O^tBu)₁₂Cl][U-(CH₂SiMe₃)₃] (U–C = 2.445(6)–2.485(6) Å). The U–C–Si

Scheme 1. Synthesis of Complexes 1 and 2



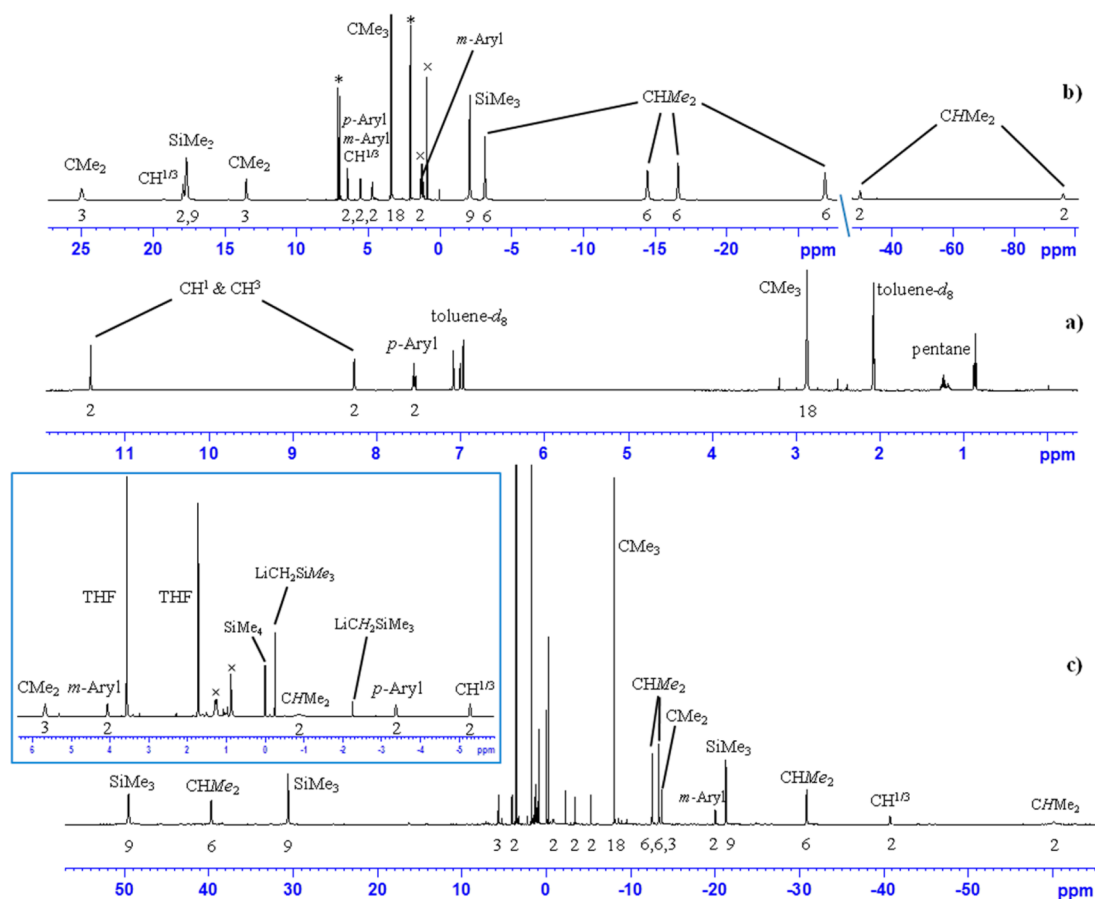


Figure 2. ^1H NMR spectra (500 MHz): (a) $[(\text{XA}_2)\text{U}(\text{CH}_2\text{SiMe}_3)_2]$ (**1**) in toluene- d_8 at room temperature; (b) complex **1** in toluene- d_8 at -60°C ; and (c) in situ generated $[\text{Li}(\text{THF})_x][(\text{XA}_2)\text{U}(\text{CH}_2\text{SiMe}_3)_3]$ (**3**) in THF- d_8 at -50°C . In the figure, * denotes toluene- d_8 and \times denotes *n*-pentane. Numbers below the baseline indicate the integration of each peak. Signals for U-CH $_2$ protons, which are located at very high (>100 ppm) and very low (<-100 ppm) frequencies in spectra b and c, are not shown. The CMe $_3$ peaks are truncated in all three spectra, and the inset shows a portion of spectrum c.

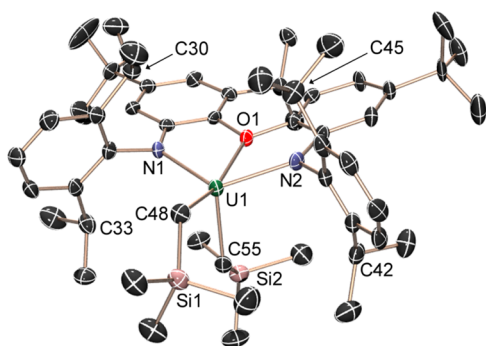


Figure 3. X-ray crystal structure of $[(\text{XA}_2)\text{U}(\text{CH}_2\text{SiMe}_3)_2] \cdot 2(n\text{-hexane})$ (**1·2(n-hexane)**) with thermal ellipsoids at the 30% probability level (collected at 173 K). Only one of the two independent molecules in the unit cell is shown. Hydrogen atoms and hexane solvent are omitted for clarity.

angles of $128.2(3)$ – $130.8(3)^\circ$ are in line with previously reported values ($125.7(3)$ – $130.6(3)^\circ$), and the U–N distances are unremarkable.²¹ However, as previously discussed in the context of $[(\text{XA}_2)\text{UCl}_3\{\text{K}(\text{dme})_3\}]$, $[(\text{XA}_2)\text{UCl}(\text{dme})]$ ²¹ and $[(\text{XA}_2)\text{Th}(\text{CH}_2\text{SiMe}_3)_2]$ (**1-Th**),³ the An–O_{xant} distances in XA $_2$ actinide complexes (2.484(5) and 2.504(4) Å in **1**) are invariably shorter than might be expected for actinide–diaryl

ether linkages, presumably due to steric constraints imposed by the rigid ligand framework.

The geometry of **1** is analogous to that of the thorium analogue, **1-Th**,^{3,22} although the An–C, An–N, and An–O distances in **1** are slightly shorter (Table 1), consistent with the smaller size of uranium (the six-coordinate ionic radii for U $^{4+}$ and Th $^{4+}$ are 0.89 and 0.94 Å, respectively).²³ In addition, the xanthene backbone in **1** deviates further from planarity (the angles between the two aryl rings of the xanthene backbone are 17.6 and 19.0° for **1** versus 9.0° for **1-Th**), and uranium is positioned further from the NON donor plane (0.64 and 0.65 Å for **1** versus 0.48 Å for **1-Th**). However, the N1⋯N2 distance in **1** is only slightly shorter than that in the thorium analogue (4.00 and 4.02 Å in **1** versus 4.06 Å in **1-Th**), and the extent to which the 2,6-diisopropylphenyl groups are rotated away from the axial alkyl group are similar in **1** and **1-Th** (C(33)⋯C(42) = 7.63 and 7.70 Å and C(30)⋯C(45) = 4.63 and 4.86 Å in **1**; the corresponding distances in **1-Th** are 7.51 and 5.00 Å).

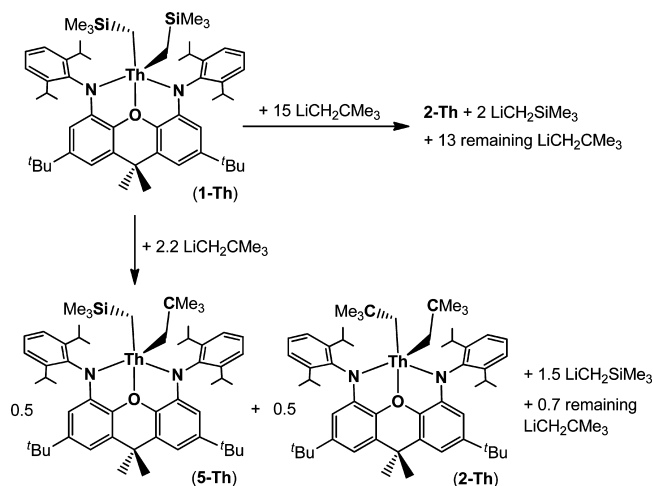
Addition of 2.1 equiv of LiCH $_2$ CMe $_3$ to $[(\text{XA}_2)\text{U}(\text{CH}_2\text{SiMe}_3)_2]$ (**1**) in C $_6$ D $_6$ resulted in quantitative conversion to $[(\text{XA}_2)\text{U}(\text{CH}_2\text{CMe}_3)_2]$ (**2**) with release of 2 equiv of LiCH $_2$ SiMe $_3$ (Scheme 1). Treatment of complex **2** with up to 80 equiv of LiCH $_2$ SiMe $_3$ in C $_6$ D $_6$ did not re-form detectable amounts of **1** by ^1H NMR spectroscopy; thus, the equilibrium in this reaction must lie far to the side of complex **2**. This unusual reaction bears a resemblance to salt metathesis (both

Table 1. Selected Bond Lengths (Å) and Angles (deg) for XA_2 Complexes **1**, **2**, and **4** as Well as the Previously Reported **1-Th** and $[(\text{XA}_2)\text{UCl}_3\{\text{K}(\text{dme})_3\}]$

	$(\text{XA}_2)\text{Th}(\text{CH}_2\text{SiMe}_3)_2$ (1-Th)	$(\text{XA}_2)\text{U}(\text{CH}_2\text{SiMe}_3)_2$ (1)	$(\text{XA}_2)\text{U}(\text{CH}_2\text{CMe}_3)_2$ (2)	$(\text{XA}_2)\text{UMe}_3$ anion (4)	$(\text{XA}_2)\text{UCl}_3\text{K}(\text{dme})_3$
lattice solvent	toluene	2 <i>n</i> -hexane	<i>n</i> -hexane	dme	none
ref	3	this work	this work	this work	21
An–O	2.535(4)	2.484(5), 2.504(4)	2.528(5), 2.529(5)	2.517(5)	2.465(3)
An–N	2.291(4), 2.312(4)	2.261(5), 2.262(5), 2.272(5), 2.280(5)	2.260(6), 2.272(6), 2.279(5), 2.289(6)	2.363(6), 2.373(6)	2.297(4), 2.306(4)
An–C _{axial} or An–Cl _{axial}	2.467(6)	2.368(7), 2.380(7)	2.386(8), 2.396(7)	U–C48: 2.377(9) U–C50: 2.493(8)	U–Cl2: 2.620(2), 2.625(2) U–Cl3: 2.629(2), 2.628(2)
An–C _{in plane} or An–Cl _{in plane}	2.484(6)	2.393(7), 2.418(7)	2.409(7), 2.417(7)	U–C49: 2.506(9)	U–Cl1: 2.632(2), 2.619(3)
An–C–C _{axial} or An–C–Si _{axial}	126.8(3)	128.2(3), 130.4(3)	134.3(5), 134.4(5)	n/a	n/a
An–C–C _{in plane} or An–C–Si _{in plane}	127.6(3)	130.5(4), 130.8(3)	130.3(5), 130.3(5)	n/a	n/a
C–An–C or Cl–An–Cl	111.9(2)	103.2(2), 105.0(2)	105.1(2), 106.6(3)	C48–U–C49: 84.2(3) C49–U–C50: 85.7(3) C48–U–C50: 169.9(3)	Cl1–U–Cl2: 89.91(6) Cl1–U–Cl3: 88.25(6) Cl2–U–Cl3: 177.07(6)
N–An–N	123.8 (2)	123.7(2), 124.0(2)	120.8(2), 120.9(2)	124.8(2)	129.1(1)
N–An–O	62.9(1), 63.0(1)	63.9(2), 64.0(2), 64.2(2), 64.4(2)	64.4(2), 64.5(2), 64.7(2), 65.1(2)	63.7(2), 63.8(2)	64.9(1), 65.5(1)
N–An–C _{axial} or N–An–Cl _{axial}	100.6(3), 100.8(2)	101.0(2), 101.6(2), 103.2(2), 103.3(2)	103.6(2), 105.5(2), 105.8(2), 108.5(2)	N–U–C48: 92.4(2), 93.1(2) N–U–C50: 90.5(2), 93.3(2)	N–U–Cl2: 89.2(1), 92.5(1) N–U–Cl3: 89.6(1), 90.3(1)
N–An–C _{in plane} or N–An–Cl _{in plane}	109.1(2), 109.7(2)	108.1(2), 110.8(2), 111.7(2), 112.5(2)	107.6(2), 108.3(2), 109.2(2), 109.8(2)	N–U–C49: 114.8(3), 120.3(3)	N–U–Cl1: 114.6(1), 116.2(1)
O–(N/An/N-plane)	0.66	0.92	1.23, 1.29	0.75	0.53
An–(N/O/N-plane)	0.48	0.64, 0.65	0.84, 0.87	0.54	0.34
angle between xanthene aromatic rings	9.0	17.6, 19.0	33.4, 34.2	6.5	1.2
C(30)⋯C(45) or analogous in 1-Th	4.00	4.63, 4.86	4.16, 4.22	7.30	6.87
C(33)⋯C(42) or analogous in 1-Th	7.51	7.63, 7.70	8.01, 8.07	6.11	6.35
N(1)⋯N(2)	4.06	4.00, 4.02	3.95, 3.96	4.20	4.16

alkyl exchange and salt metathesis are classes of transmetalation reactions), but with elimination of $\text{LiCH}_2\text{SiMe}_3$ instead of a lithium halide. It is not unique to uranium, since the reaction between **1-Th** and 15 equiv of $\text{LiCH}_2\text{CMe}_3$ cleanly provided $[(\text{XA}_2)\text{Th}(\text{CH}_2\text{CMe}_3)_2]$ (**2-Th**; Figure S5 (Supporting Information)). However, addition of 2.2 equiv of $\text{LiCH}_2\text{CMe}_3$ to **1-Th** yielded an approximate 1:1:3:1 mixture of **2-Th**, $[(\text{XA}_2)\text{Th}(\text{CH}_2\text{SiMe}_3)(\text{CH}_2\text{CMe}_3)]$ (**5-Th**), $\text{LiCH}_2\text{SiMe}_3$, and $\text{LiCH}_2\text{CMe}_3$ (Scheme 2 and Figure S4 (Supporting Information)). This product distribution was established within 5 min and did not change with extended reaction times (days), consistent with a significantly smaller equilibrium constant for the reaction of **1-Th** with $\text{LiCH}_2\text{CMe}_3$, relative to the reaction of uranium complex **1** with $\text{LiCH}_2\text{CMe}_3$. Complex **5-Th** is the mixed alkyl species that must form en route from **1-Th** to **2-Th**, and both **2-Th** and **5-Th** were characterized in situ by ^1H , ^{13}C , and 2D NMR spectroscopy (at low temperature for **2-Th**).

Complex **2** could also be prepared by a traditional salt metathesis reaction between $[(\text{XA}_2)\text{UCl}_3\{\text{K}(\text{dme})_3\}]$ and 2 equiv of $\text{LiCH}_2\text{CMe}_3$ (Scheme 1), and dark red crystals of **2** (*n*-hexane) were obtained from a concentrated hexanes solution at -30°C . Many of the peaks in the room-temperature ^1H NMR spectrum of **2** are extremely broad, indicative of a fluxional process which exchanges the axial and in-plane alkyl groups, but as for complex **1**, a sharp spectrum consistent with C_s symmetry was observed at low temperature (Figure 4).

Scheme 2. Reactions of **1-Th** with 2.2 and 15 equiv of $\text{LiCH}_2\text{CMe}_3$ 

The solid-state geometry of complex **2** (Figure 5 and Table 1) is analogous to that of **1**, and as with **1**, there are two independent but structurally analogous molecules in the unit cell. The U–C and U–N distances are comparable with those in **1**, despite the increased basicity of CH_2CMe_3 groups relative to CH_2SiMe_3 groups,²⁴ and the U–O distances are only

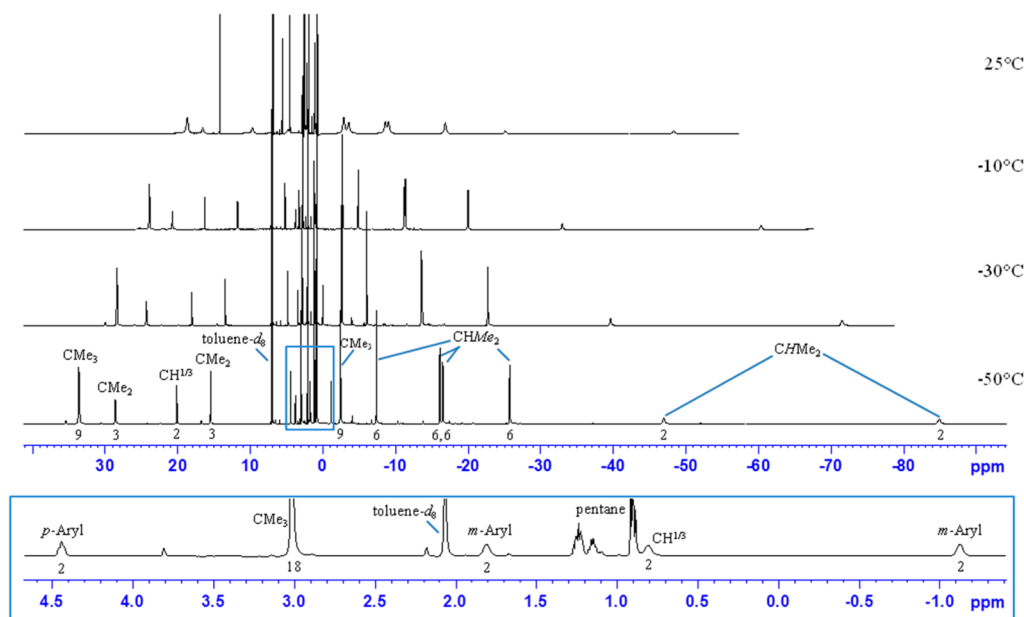


Figure 4. 500 MHz ^1H NMR spectra of $[(\text{XA}_2)\text{U}(\text{CH}_2\text{CMe}_3)_2]$ (**2**) in toluene- d_8 at temperatures from 25 to -50°C . Numbers below the baseline indicate the integration of each peak. Signals for $\text{U}-\text{CH}_2$ protons, which are located at very high (>100 ppm) and very low (<-100 ppm) frequencies, are not shown. The inset at the bottom shows a portion of the -50°C spectrum.

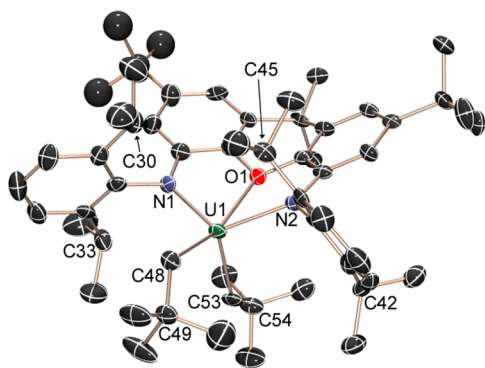


Figure 5. X-ray crystal structure of $[(\text{XA}_2)\text{U}(\text{CH}_2\text{CMe}_3)_2] \cdot (n\text{-hexane})$ (**2**·(*n*-hexane)) with thermal ellipsoids at the 50% probability level (collected at 100 K). Only one of the two independent molecules in the unit cell is shown. Hydrogen atoms and hexane solvent are omitted for clarity. One *tert*-butyl group is disordered and so was refined isotropically, and only one of the two orientations of the disordered *tert*-butyl group is shown.

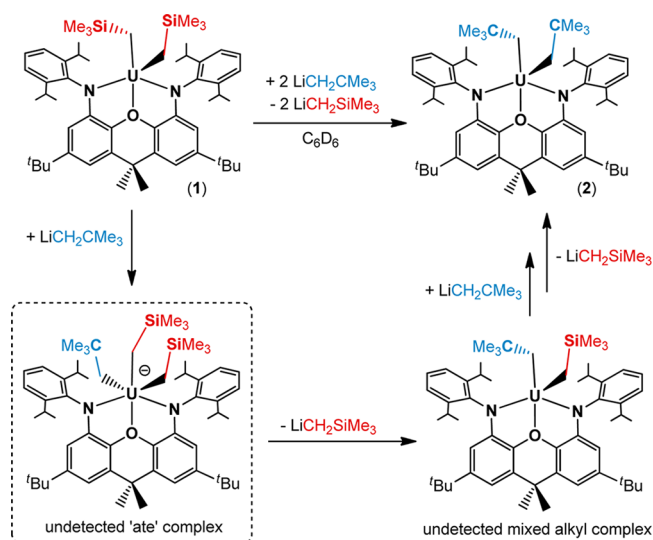
marginally longer than those in **1**. However, due to the increased steric presence of the neopentyl anion, uranium is located further from the NON donor plane in complex **2** (0.84 and 0.87 Å versus 0.64 and 0.65 Å in **1**), and the neutral oxygen donor is located further (1.23 and 1.29 Å versus 0.92 and 0.95 Å in **1**) from the NUN plane. In addition, the ligand backbone deviates further from planarity (the angles between the aromatic rings in the xanthene backbone are 33.4 and 34.2° versus 17.6 and 19.0° in **1**), and the 2,6-diisopropylphenyl groups are more strongly rotated away from the axial alkyl group so as to minimize unfavorable steric interactions: $\text{C}(33)\cdots\text{C}(42) = 8.01$ and 8.07 Å and $\text{C}(30)\cdots\text{C}(45) = 4.16$ and 4.22 Å (cf. $\text{C}(33)\cdots\text{C}(42) = 7.63$ and 7.70 Å and $\text{C}(30)\cdots\text{C}(45) = 4.63$ and 4.86 Å in **1**).

Dialkyl complexes **1** and **2** are thermally stable for days at room temperature in aromatic solvents. However, over the course of several days at 45°C , **1** and **2** were converted to a

mixture of unidentified paramagnetic products with concomitant evolution of SiMe_4 or CMe_4 , respectively. Upon further heating at $60\text{--}80^\circ\text{C}$ for 24–48 h, **1** and **2** were fully decomposed to give spectra dominated by SiMe_4 or CMe_4 (at this point, ^1H NMR signals attributable to diamagnetic or paramagnetic XA_2 ligand-containing products were low in intensity). We have previously reported similar behavior for the decomposition of $[(\text{XA}_2)\text{Th}(\text{CH}_2\text{SiMe}_3)_2]$ (**1-Th**) at 90°C .³

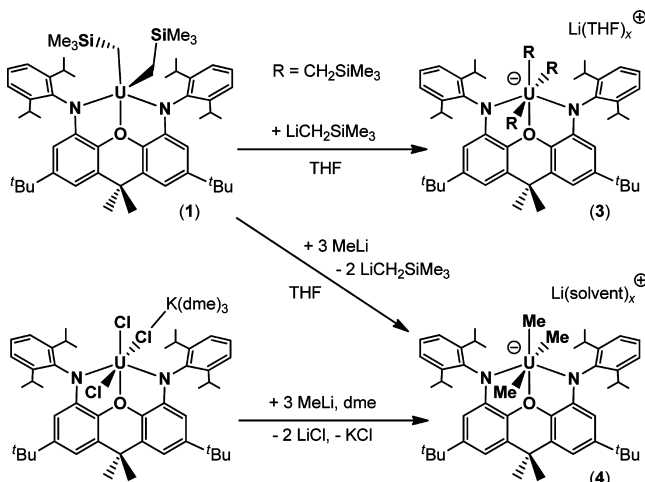
The reaction to convert **1** to **2** presumably occurs via trialkyl “ate” intermediates, as shown in Scheme 3. These intermediates were not detected in the reaction of **1** with $\text{LiCH}_2\text{CMe}_3$ in aromatic solvents, and reaction of complex **1** with up to 20 equiv of $\text{LiCH}_2\text{SiMe}_3$ in C_6D_6 did not provide any evidence for the formation of $[(\text{XA}_2)\text{U}(\text{CH}_2\text{SiMe}_3)_3]^-$ by ^1H NMR spectroscopy. However, trialkyl “ate” complexes did prove

Scheme 3. Proposed Reaction Pathway for the Conversion of **1** to **2**



accessible in THF; addition of 1.3 equiv of $\text{LiCH}_2\text{SiMe}_3$ to **1** in THF yielded $[\text{Li}(\text{THF})_x][(\text{XA}_2)\text{U}(\text{CH}_2\text{SiMe}_3)_3]$ (**3**), which was characterized in situ by variable-temperature ^1H NMR spectroscopy (Figure 2), and addition of 3.3 equiv of MeLi to **1** in THF cleanly afforded $[\text{Li}(\text{THF})_x][(\text{XA}_2)\text{UMe}_3]$ (**4**; Scheme 4 and Figure S6 (Supporting Information)). Hexane-insoluble

Scheme 4. Synthesis of Complexes **3** and **4**



$[\text{Li}(\text{dme})_3][(\text{XA}_2)\text{UMe}_3]$ (**4**; Scheme 4) could also be prepared from the reaction of $[(\text{XA}_2)\text{UCl}_3\{\text{K}(\text{dme})_3\}]$ with 3 equiv of MeLi in *dme*. In contrast, reactions of **1** or $[(\text{XA}_2)\text{UCl}_3\{\text{K}(\text{dme})_3\}]$ with 2 equiv of MeLi in *dme* or THF yielded mixtures of unidentified products. Anionic **3** and **4** are less thermally stable than neutral **1** and **2**, decomposing over several days at room temperature in THF to produce a mixture of unidentified paramagnetic products accompanied by SiMe_4 or CH_4 , respectively.

The room-temperature ^1H NMR spectrum of **4** in $\text{THF}-d_8$ is consistent with a top–bottom-symmetric environment (C_{2v} symmetry) on the NMR time scale. Golden yellow X-ray-quality crystals of **4-dme** were obtained from *dme*/hexanes at -30°C ; the ligand backbone in six-coordinate **4** (Figure 6) is

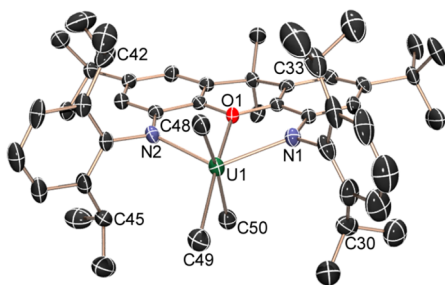


Figure 6. X-ray crystal structure of $[\text{Li}(\text{dme})_3][(\text{XA}_2)\text{UMe}_3]\cdot\text{dme}$ (**4-dme**) with thermal ellipsoids at 30% (collected at 173 K). Hydrogen atoms, *dme* lattice solvent, and the $\text{Li}(\text{dme})_3^+$ cation are omitted for clarity.

approximately planar (the angle between the two aryl rings of the xanthene backbone is 6.5°), uranium is located 0.54 \AA from the NON donor plane, the five anionic donors in **4** form a trigonal bipyramid (we are not suggesting that **4** is five-coordinate) with methyl groups in axial positions, and the neutral donor is located 0.75 \AA out of the NUN plane in the direction of C(50). The U–N distances are approximately 0.1

\AA longer than those in complexes **1** and **2**, and only the U–C(48) distance of $2.377(9)\text{ \AA}$ falls within the range observed for the U–C bonds in **1** and **2**; the U–C(49) and U–C(50) bonds in **4** are substantially longer at $2.493(8)$ and $2.506(9)\text{ \AA}$. The elongated uranium–ligand bond lengths in **4** can be explained on the basis of an increased coordination number at uranium and an overall anionic charge on the complex. The geometry of complex **4** is analogous to that in six-coordinate $[(\text{XA}_2)\text{UCl}_3\{\text{K}(\text{dme})_3\}]$, which also exhibits a planar xanthene backbone and a trigonal-bipyramidal arrangement of the anionic donors. However, the U–O and U–N distances in **4** are substantially longer than those in $[(\text{XA}_2)\text{UCl}_3\{\text{K}(\text{dme})_3\}]$ (Table 1), most likely due to decreased Lewis acidity, increased steric hindrance, and complete separation of the anionic portion of the complex from the alkali-metal counterion in **4**.

The extent to which the reactions of **1** with 2.1 equiv of $\text{LiCH}_2\text{CMe}_3$ (in benzene) or 3.3 equiv of MeLi (in THF) lie toward the side of the products (**2** or **4** and $\text{LiCH}_2\text{SiMe}_3$) is remarkable and likely²⁵ reflects the increased basicity of neopentyl and methyl anions in comparison with the (trimethylsilyl)methyl anion,²⁴ leading to stronger uranium–alkyl bonds. The requirement for addition of more than 2 equiv of $\text{LiCH}_2\text{CMe}_3$ to convert **1-Th** to **2-Th** is also intriguing in that it highlights distinct differences in the reactivity of thorium and uranium.

Previously reported alkyl exchange reactions at electro-positive d- or f-element centers include (1) synthesis of $[\{o\text{-C}_6\text{H}_4(\text{N-Dipp})(\text{PPh}(\text{C}_6\text{H}_4)(=\text{N-Mes}))\}\text{LuMe}(\text{THF})_2]$ by treatment of $[\{o\text{-C}_6\text{H}_4(\text{N-Dipp})(\text{PPh}(\text{C}_6\text{H}_4)(=\text{N-Mes}))\}\text{Lu}(\text{CH}_2\text{SiMe}_3)(\text{THF})]$ with 10 equiv of AlMe_3 in THF,²⁶ (2) reaction of $[\text{Me}_2\text{Si}(2\text{-Me-C}_9\text{H}_5)_2]\text{YMe}(\text{THF})]$ with AlEt_3 followed by addition of THF to yield an approximately 1:1 mixture of the starting methyl complex and $[\text{Me}_2\text{Si}(2\text{-Me-C}_9\text{H}_5)_2]\text{YEt}(\text{THF})]$,²⁷ and (3) exchange between a growing polymer chain on a d- or f-element polymerization catalyst and the alkyl group of an added trialkylaluminum,^{28–31} trialkylboron,³² dialkylzinc^{30,31,33} or dialkylmagnesium³⁴ reagent. This last mode of reactivity³⁵ is typically detrimental to olefin polymerization activity³⁵ but has found productive use in chain-shuttling alkene polymerization³³ and metal-catalyzed “Aufbaureaktion” chemistry.^{28,31} Alkyl exchange reactions involving alkyl lithium reactions are more scarce but have been reported for dialkylmercury compounds in combination with alkyl-lithium reagents; these reactions proceed to completion when the alkyl lithium product is insoluble in the solvent employed.³⁶

The alkyl exchange reactions in this work also bear resemblance to salt metathesis-like reactions involving cyclopentadienyl anion elimination from polar metallocenes. These include the reaction of $[\{\text{Cp}^*\text{U}\}_2(\mu\text{-}\eta^6\text{-}\eta^6\text{-C}_6\text{H}_6)]$ with MX ($\text{M} = \text{K}$, $\text{X} = \text{N}(\text{SiMe}_3)_2$, $\text{OC}_6\text{H}_2(\text{CMe}_3)_2\text{-2,6-Me-4}$; $\text{M} = \text{Li}$, $\text{X} = \text{CH}(\text{SiMe}_3)_2$, $^i\text{PrNCMeN}^i\text{Pr}$) to form $[\{\text{Cp}^*\text{XU}\}_2(\mu\text{-}\eta^6\text{-}\eta^6\text{-C}_6\text{H}_6)]$,³⁷ reaction of $[\text{MnCp}_2]$ with LiC_2Ph in THF to provide $0.5 [\{\text{CpMn}(\mu\text{-C}_2\text{Ph})(\text{THF})\}_2]$,³⁸ reaction of $[\text{MnCp}_2]$ with 1 or 3 equiv of $\text{Li}(\text{hpp})$ to afford $0.5 [\{\text{CpMn}(\text{hpp})\}_2]$ or $[\{\text{LiMn}(\text{hpp})_3\}_2]$,³⁹ reaction of $[\text{VCp}_2]$ with 2 equiv of $\text{Li}(\text{hpp})$ to give $0.25 [\{\text{V}_2(\text{hpp})_4\}\text{Li}(\mu\text{-Cp})\text{Li}(\mu\text{-Cp})\text{Li}(\text{V}_2(\text{hpp})_4)]\text{-}[\text{CpLi}(\mu\text{-Cp})\text{LiCp}]$,⁴⁰ and reaction of $[\text{CrCp}_2]$ with 2 equiv of $\text{Li}(\text{MeNCHNMe})$ to yield $0.5 [\text{Cr}_2(\text{MeNCHNMe})_4]$.⁴¹

SUMMARY AND CONCLUSIONS

The preparation and crystallographic characterization of $[(\text{XA}_2)\text{U}(\text{CH}_2\text{SiMe}_3)_2]$ (**1**), $[(\text{XA}_2)\text{U}(\text{CH}_2\text{CMe}_3)_2]$ (**2**), and $[(\text{XA}_2)\text{UMe}_3]^-$ (**4**) and in situ syntheses of $[(\text{XA}_2)\text{U}$

$(\text{CH}_2\text{SiMe}_3)_3^-$ (**3**), $[(\text{Xa}_2)\text{Th}(\text{CH}_2\text{CMe}_3)_2]$ (**2-Th**), and $[(\text{Xa}_2)\text{Th}(\text{CH}_2\text{SiMe}_3)(\text{CH}_2\text{CMe}_3)]$ (**5-Th**) are reported. Reaction of **1** with 2.1 equiv of $\text{LiCH}_2\text{CMe}_3$ in benzene resulted in rapid conversion to **2** and 2 equiv of $\text{LiCH}_2\text{SiMe}_3$. This unusual exchange reaction resembles salt metathesis and presumably proceeds via undetected trialkyl “ate” intermediates. Reactions of this type may find utility for clean in situ generation of new alkyl complexes but are only likely to be of preparative value if the solubility of the alkyl lithium byproduct permits its complete removal. The generality of this type of alkyl exchange reaction also remains to be determined. However, it is notable that while the reaction of **1** with 2.1 equiv of $\text{LiCH}_2\text{CMe}_3$ proceeds quantitatively to the dineopentyl complex, the analogous reaction of $[(\text{Xa}_2)\text{Th}(\text{CH}_2\text{SiMe}_3)_2]$ (**1-Th**) requires a significant excess of $\text{LiCH}_2\text{CMe}_3$ to reach completion.

EXPERIMENTAL SECTION

General Details. General synthetic procedures have been reported elsewhere.^{3,16,17,19,42} Deuterated solvents were purchased from ACP Chemicals. Neopentyl chloride was purchased from Strem Chemicals. $\text{LiCH}_2\text{SiMe}_3$ (1.0 M in *n*-pentane) and MeLi (1.60 M in OEt_2) solutions were purchased from Sigma-Aldrich, and prior to use, solid $\text{LiCH}_2\text{SiMe}_3$ and MeLi were obtained by removal of solvent in vacuo. $\text{H}_2[\text{Xa}_2]$,³ UCl_4 ,⁴³ $[(\text{Xa}_2)\text{UCl}_3\{\text{K}(\text{dme})_3\}]$,²¹ $[(\text{Xa}_2)\text{Th}(\text{CH}_2\text{SiMe}_3)_2]$ (**1-Th**),³ and $\text{LiCH}_2\text{CMe}_3$ ⁴⁴ were prepared using literature procedures. In situ reactions to form **2** (method 2), **3**, **4** (method 2), and **5-Th** involved the use of small amounts (3.0–0.7 mg) of alkyl lithium reagents. These reagents were weighed out as accurately as possible using an analytical balance (accurate to 0.1 mg), but the actual reported stoichiometries of these reactions were determined by ^1H NMR integration. Sonication was employed in several NMR tube reactions in lieu of stirring. If sonication was continued for extended periods of time, the water in the sonicator was changed periodically (approximately every 30 min) to prevent undesired heating of the reaction.

Combustion elemental analyses were performed on a Thermo EA1112 CHNS/O analyzer by Ms. Meghan Fair or Dr. Steve Kornic of this department. X-ray crystallographic analyses were performed on suitable crystals coated in Paratone oil and mounted on a SMART APEX II diffractometer with a 3 kW sealed-tube Mo generator at the McMaster Analytical X-ray (MAX) Diffraction Facility. Three of four molecules of *n*-hexane in the unit cell of **1-2**(*n*-hexane) (*Z* = 2), and two molecules of *n*-hexane in the unit cell of **2**·(*n*-hexane) (*Z* = 2) were highly disordered and could not be modeled satisfactorily and so were treated using the SQUEEZE routine.⁴⁵ ^1H , $^{13}\text{C}\{^1\text{H}\}$, DEPT-q, COSY, HSQC, and HMBC NMR spectroscopy was performed on Bruker AV-200, DRX-500, and AV-600 spectrometers. All ^1H NMR spectra were referenced relative to SiMe_4 through a resonance of the employed deuterated solvent or protio impurity of the solvent: C_6D_6 (7.16 ppm), C_7D_8 (7.09, 7.01, 6.97, 2.08 ppm), and THF-d_8 (3.58, 1.73 ppm) for ^1H NMR, and C_6D_6 (128.0 ppm), C_7D_8 (137.48, 128.87, 127.96, 125.13, 20.43 ppm), and THF-d_8 (67.57, 25.37 ppm) for ^{13}C NMR.

All NMR spectra were obtained at room temperature unless otherwise specified. Herein, Aryl = 2,6-diisopropylphenyl, and the numbering scheme ($\text{CH}^{1,8}$, $\text{C}^{2,7}$, $\text{CH}^{3,6}$, $\text{C}^{4,5}$, $\text{C}^{10/13}$, and $\text{C}^{11,12}$) for the xanthene ligand backbone is shown in Scheme 1. Most peaks in the ^1H NMR spectra of paramagnetic uranium(IV) complexes could be assigned on the basis of integration. The para aryl, $\text{CH}^{1,8}$, $\text{CH}^{3,6}$, and *tert*-butyl signals were also readily identified, since they are unaffected by the presence/absence of top–bottom symmetry on the NMR time scale. Furthermore, the para Ar signal always appeared as a triplet at room temperature, allowing definite assignment. The broad signals integrating to 2H and located between –25 and –100 ppm in the spectra of **1** and **2** were speculatively assigned as the isopropyl methine protons (rather than the meta aryl protons), given their close proximity to the paramagnetic U(IV) center.

$[(\text{Xa}_2)\text{U}(\text{CH}_2\text{SiMe}_3)_2]$ (**1**). A mixture of $[(\text{Xa}_2)\text{UCl}_3\{\text{K}(\text{dme})_3\}]$ (0.150 g, 0.11 mmol) and $\text{LiCH}_2\text{SiMe}_3$ (0.022 g, 0.24 mmol) in hexanes (20 mL) was stirred at -78°C and then warmed slowly to room temperature; stirring was continued for a total of 12 h. The orange-red solution was evaporated to dryness in vacuo, and the solid residue was extracted with a minimum amount of hexanes. The suspension was centrifuged to remove insoluble KCl and LiCl, and the red mother liquors were cooled to -30°C . After a few days, X-ray-quality bright red crystals of **1-2**(*n*-hexane) were collected in two batches and dried in vacuo to provide 0.079 g of **1** (0.072 mmol, 64% yield). Alternatively, crystallization from a minimum amount of *n*-pentane at -30°C followed by drying in vacuo provided **1**·(*n*-pentane) in comparable yield. ^1H NMR (C_6D_6 , 200 MHz, 298 K): δ 12.30, 7.32 (broad s, $2 \times 2\text{H}$, $\text{CH}^{1,8}$ and $\text{CH}^{3,6}$), 7.25 (t, $^3J_{\text{H,H}} = 8\text{ Hz}$, 2H, Aryl-para), 2.82 (s, 18H, CMe_3). ^1H NMR (toluene- d_8 , 500.1 MHz, 298 K): δ 11.41, 8.27 (broad s, $2 \times 2\text{H}$, $\text{CH}^{1,8}$ and $\text{CH}^{3,6}$), 7.56 (t, $^3J_{\text{H,H}} = 9.3\text{ Hz}$, 2H, Aryl-para), 2.87 (s, 18H, CMe_3). UCH_2 protons were not observed at room temperature. ^1H NMR (toluene- d_8 , 500.1 MHz, 213 K): δ 178.2, –222.3 (extremely broad s, $2 \times 2\text{H}$, UCH_2), 25.00, 13.51 (broad s, $2 \times 3\text{H}$, CMe_2), 17.93, 4.71 (broad s, $2 \times 2\text{H}$, $\text{CH}^{1,8}$ and $\text{CH}^{3,6}$), 17.69, –2.08 (broad s, $2 \times 9\text{H}$, SiMe_3), 6.45 (broad s, 2H, Aryl-para), 5.54, 1.33 (broad s, $2 \times 2\text{H}$, Aryl-meta), 3.40 (s, 18H, CMe_3), –3.14, –14.47, –16.61, –26.85 (broad s, $4 \times 6\text{H}$, CHMe_2), –29.86, –96.02 (v broad s, $2 \times 2\text{H}$, CHMe_2). Anal. Calcd for $\text{C}_{55}\text{H}_{84}\text{N}_2\text{OSi}_2\text{U}$: C, 60.97; H, 7.81; N, 2.59. Found: C, 61.05; H, 8.06; N, 2.38.

$[(\text{Xa}_2)\text{U}(\text{CH}_2\text{CMe}_3)_2]$ (**2**). **Method 1.** A mixture of $[(\text{Xa}_2)\text{UCl}_3\{\text{K}(\text{dme})_3\}]$ (0.250 g, 0.19 mmol) and $\text{LiCH}_2\text{CMe}_3$ (0.031 g, 0.39 mmol) in hexanes (25 mL) was stirred at -78°C and then warmed slowly to room temperature; stirring was continued for a total of 12 h. The deep red solution was evaporated to dryness in vacuo, and the solid residue was extracted with a minimum amount of *n*-pentane. The suspension was centrifuged to remove insoluble KCl and LiCl, and the deep red mother liquors were cooled to -30°C . After a few days, deep red crystals were collected in two batches and dried in vacuo to provide 0.146 g of **2**·(*n*-pentane) (0.13 mmol, 69% yield). Alternatively, crystallization from a minimum amount of hexanes at -30°C provided X-ray-quality crystals of **2**·(*n*-hexane) in comparable yield.

Method 2. Complex **2** was generated in situ by reaction of **1**·(*n*-pentane) (0.015 g, 0.013 mmol) with 2.1 equiv of $\text{LiCH}_2\text{CMe}_3$ (0.0021 g, 0.027 mmol) in C_6D_6 . After approximately 1 h of sonication, ^1H NMR indicated complete conversion of **1** to **2** (the reaction was usually complete after 20 min) with concomitant release of $\text{LiCH}_2\text{SiMe}_3$. **Method 2** was not pursued as a means to isolate pure **2**, since both **2** and $\text{LiCH}_2\text{SiMe}_3$ are highly soluble in hexanes. ^1H NMR (C_6D_6 , 500.1 MHz, 298 K): δ 141.1, –142.1 (extremely broad s, $2 \times 2\text{H}$, UCH_2), 20.02, –2.43 (v broad s, $2 \times 9\text{H}$, CH_2CMe_3), 17.51, 10.17 (v broad s, $2 \times 3\text{H}$, CMe_2), 14.71, 4.05 (s, $2 \times 2\text{H}$, $\text{CH}^{1,8}$ and $\text{CH}^{3,6}$), 5.57 (t, $^3J_{\text{H,H}} = 8\text{ Hz}$, 2H, Aryl-para), 4.42, 2.02 (v broad s, $2 \times 2\text{H}$, Aryl-meta), 2.61 (s, 18H, CMe_3), –3.89, –9.21, –18.84 (v broad s, $4 \times 6\text{H}$, CHMe_2), –27.15, –49.21 (v broad s, $2 \times 2\text{H}$, CHMe_2). ^1H NMR (toluene- d_8 , 500.1 MHz, 298 K): δ 134.5, –138.8 (extremely broad s, $2 \times 2\text{H}$, UCH_2), 18.78, –2.77 (v broad s, $2 \times 9\text{H}$, CH_2CMe_3), 16.66, 9.80 (v broad s, $2 \times 3\text{H}$, CMe_2), 14.26, 4.63 (s, $2 \times 2\text{H}$, $\text{CH}^{1,8}$ and $\text{CH}^{3,6}$), 5.71 (t, $^3J_{\text{H,H}} = 8.6\text{ Hz}$, 2H, Aryl-para), 4.88, 2.29 (v broad s, $2 \times 2\text{H}$, Aryl-meta), 2.66 (s, 18H, CMe_3), –3.43, –8.48, –8.92, –16.73 (v broad s, $4 \times 6\text{H}$, CHMe_2), –24.98, –48.17 (v broad s, $2 \times 2\text{H}$, CHMe_2). ^1H NMR (toluene- d_8 , 500.1 MHz, 223 K): δ 223.3, –221.5 (extremely broad s, $2 \times 2\text{H}$, UCH_2), 33.64, –2.39 (broad s, $2 \times 9\text{H}$, CH_2CMe_3), 28.61, 15.47 (broad s, $2 \times 3\text{H}$, CMe_2), 20.13, 0.81 (broad s, $2 \times 2\text{H}$, $\text{CH}^{1,8}$ and $\text{CH}^{3,6}$), 4.45 (broad t, 2H, Aryl-para), 3.02 (s, 18H, CMe_3), 1.81, –1.12 (broad s, $2 \times 2\text{H}$, Aryl-meta), –7.35, –16.10, –16.48, –25.70 (broad s, $4 \times 6\text{H}$, CHMe_2), –46.92, –84.92 (v broad s, $2 \times 2\text{H}$, CHMe_2). Anal. Calcd for $\text{C}_{62}\text{H}_{96}\text{N}_2\text{OU}$: C, 66.28; H, 8.61; N, 2.49. Found: C, 66.76; H, 8.01; N, 2.39.

$[\text{Li}(\text{THF})_x][(\text{Xa}_2)\text{U}(\text{CH}_2\text{SiMe}_3)_2]$ (**3**; in Situ). A mixture of $[(\text{Xa}_2)\text{U}(\text{CH}_2\text{SiMe}_3)_2]$ ·(*n*-pentane) (**1**·(*n*-pentane); 0.010 g, 0.009 mmol) and 1.3 equiv of $\text{LiCH}_2\text{SiMe}_3$ (0.0011 g, 0.011 mmol) were taken up in THF- d_8 to afford a yellow solution. Five minutes after

mixing, ^1H NMR revealed new signals corresponding to **3**, with concomitant loss of **1**. ^1H NMR (THF- d_8 , 500.1 MHz, 298 K): δ 314.6, 268.8, -161.0 (extremely broad s, $3 \times 2\text{H}$, UCH_2), 35.08, 23.20, -14.20 (v broad s, $3 \times 9\text{H}$, CH_2SiMe_3), 28.34, -9.54, -11.39, -24.50 (v broad s, $4 \times 6\text{H}$, CHMe_2), 5.85, -12.40 (v broad s, $2 \times 2\text{H}$, Aryl-meta), 4.70, -9.50 (v broad s, $2 \times 3\text{H}$, CMe_2), 0.19 (t, $^3J_{\text{H,H}} = 7$ Hz, 2H , Aryl-para), -1.49, -28.03 (s, $2 \times 2\text{H}$, $\text{CH}^{1,8}$ and $\text{CH}^{3,6}$), -1.65, -56.37 (v broad s, $2 \times 2\text{H}$, CHMe_2), -5.34 (s, 18H , CMe_3). ^1H NMR (THF- d_8 , 500.1 MHz, 223 K): δ 451.0, 378.0, -236.9 (extremely broad s, $3 \times 2\text{H}$, UCH_2), 49.48, 30.58, -21.27 (broad s, $3 \times 9\text{H}$, CH_2SiMe_3), 39.69, -12.53, -13.32, -30.85 (broad s, $4 \times 6\text{H}$, CHMe_2), 5.68, -13.68 (broad s, $2 \times 3\text{H}$, CMe_2), 4.07, -20.03 (broad s, $2 \times 2\text{H}$, Aryl-meta), -0.86, -60.16 (v broad s, $2 \times 2\text{H}$, CHMe_2), -3.37 (broad s, 2H , Aryl-para), -5.28, -40.72 (broad s, $2 \times 2\text{H}$, $\text{CH}^{1,8}$ and $\text{CH}^{3,6}$), -8.04 (s, 18H , CMe_3).

[Li(dme)₃][(XA₂)UMe₃] (4). *Method 1.* A mixture of $[(\text{XA}_2\text{UCl}_3\{\text{K}(\text{dme})_3\})]$ (0.150 g, 0.11 mmol) and MeLi (0.008 g, 0.37 mmol) in dme (20 mL) was stirred at -78°C and then warmed slowly to room temperature; stirring was continued for a total of 12 h. The yellow solution was evaporated to dryness in vacuo, and the solid residue was extracted with toluene (20 mL). The suspension was filtered to remove insoluble KCl and LiCl, and the yellow filtrate was evaporated to dryness in vacuo. The solid residue was taken up in minimal dme and layered with hexanes. After a few days at -30°C , X-ray-quality crystals of **4**-dme were obtained and dried in vacuo to provide 0.046 g of **4**-dme (0.035 mmol, 31% yield). The low yield likely results from losses during extraction as a consequence of poor solubility in toluene.

Method 2. Complex **4** can be prepared cleanly in situ by reaction of **1**-(*n*-pentane) (0.010 g, 0.009 mmol) and MeLi (0.0007 g, 0.03 mmol) in THF- d_8 to afford a yellow solution. After 30 min of sonication, ^1H NMR revealed new signals corresponding to **4** with concomitant loss of **1**. ^1H NMR (THF- d_8 , 500.1 MHz, 298 K): δ 6.29, -7.04 (broad s, $2 \times 12\text{H}$, CHMe_2), -1.53 (t, $^3J_{\text{H,H}} = 6$ Hz, 2H , Aryl-para), -2.26 (s, 6H , CMe_2), -2.44, -28.86 (s, $2 \times 2\text{H}$, $\text{CH}^{1,8}$ and $\text{CH}^{3,6}$), -4.59 (v broad s, 4H , CHMe_2), -5.69 (s, 18H , CMe_3), -5.84 (d, $^3J_{\text{H,H}} = 5$ Hz, 4H , Aryl-meta). Signals corresponding to the UCH_3 protons were not located between +400 and -400 ppm. Anal. Calcd for $\text{C}_{62}\text{H}_{101}\text{N}_2\text{O}_7\text{LiU}$ prepared using method 1: C, 60.47; H, 8.27; N, 2.27. Found: C, 60.79; H, 7.73; N, 2.08.

[(XA₂)Th(CH₂SiMe₃)₂] (2-Th; in Situ). A mixture of $[(\text{XA}_2)\text{Th}(\text{CH}_2\text{SiMe}_3)_2] \cdot 0.50(\text{SiMe}_3)_2$ (**1-Th**-0.50(SiMe_3)₂) (0.020 g, 0.017 mmol) and 15 equiv of $\text{LiCH}_2\text{CMe}_3$ (0.022 g, 0.26 mmol) were taken up in toluene- d_8 to afford a colorless solution. Five minutes after mixing, ^1H NMR revealed new signals corresponding to **2-Th** and free $\text{LiCH}_2\text{SiMe}_3$, with concomitant loss of **1-Th**. ^1H NMR (toluene- d_8 , 600.1 MHz, 298 K): δ 7.25 (broad s, 6H , Aryl-meta and Aryl-para), 6.76, 6.03 (d, $^4J_{\text{H,H}} = 2$ Hz, $2 \times 2\text{H}$, $\text{CH}^{1,8}$ and $\text{CH}^{3,6}$), 3.63 (v broad s, 4H , CHMe_2), 1.66 (s, 6H , CMe_2), 1.41, 1.15 (broad s, $2 \times 12\text{H}$, CHMe_2), 1.32 (broad s, 4H , ThCH_2), 1.18 (s, 18H , CMe_3), 0.90 (broad s, 18H , $\text{ThCH}_2\text{CMe}_3$). ^1H NMR (toluene- d_8 , 500.1 MHz, 213 K): δ 7.28 (m, $^3J_{\text{H,H}} = 7$ Hz, 4H , Aryl-meta and Aryl-para), 7.16 (d, $^3J_{\text{H,H}} = 7$ Hz, 2H , Aryl-meta), 6.79, 6.14 (s, $2 \times 2\text{H}$, $\text{CH}^{1,8}$ and $\text{CH}^{3,6}$), 4.19, 3.20 (broad sept, $^3J_{\text{H,H}} = 6.3$ Hz, $2 \times 2\text{H}$, CHMe_2), 1.74, 1.54 (broad s, $2 \times 3\text{H}$, CMe_2), 1.60, 1.36, 1.22, 1.10 (broad d, $^3J_{\text{H,H}} = 6.2$ Hz, $4 \times 6\text{H}$, CHMe_2), 1.29, 0.71 (broad s, $2 \times 9\text{H}$, $\text{ThCH}_2\text{CMe}_3$), 1.17 (broad s, 18H , CMe_3), 0.97, -0.30 (broad s, $2 \times 2\text{H}$, $\text{ThCH}_2\text{CMe}_3$). $^{13}\text{C}\{^1\text{H}\}$ NMR (toluene- d_8 , 150 MHz, 298 K): δ 148.14 ($\text{C}^{2,7}$), 147.86 (Aryl- C_{ortho}), 146.24 ($\text{C}^{4,5}$), 141.93 ($\text{C}^{1,12}$), 136.32 (Aryl- C_{ipso}), 130.02 ($\text{C}^{10,13}$), 128.04 (Aryl- C_{para}), 125.38 (Aryl- C_{meta}), 110.56, 109.89 ($\text{CH}^{1,8}$ and $\text{CH}^{3,6}$), 37.94 ($\text{ThCH}_2\text{CMe}_3$), 35.66 ($\text{ThCH}_2\text{CMe}_3$), 35.24 (CMe_2), 35.03 (CMe_3), 31.67 (CMe_3), 29.0 (CHMe_2), 26.25, 25.17 (CHMe_2). $^{13}\text{C}\{^1\text{H}\}$ NMR (toluene- d_8 , 150 MHz, 213 K): δ 147.96, 147.32 ($2 \times$ Aryl- C_{ortho}), 147.78 ($\text{C}^{2,7}$), 146.06 ($\text{C}^{4,5}$), 142.24 ($\text{C}^{1,12}$), 135.81, 120.59 ($2 \times$ $\text{ThCH}_2\text{CMe}_3$), 135.02 (Aryl- C_{ipso}), 129.91 ($\text{C}^{10,13}$), 128.18, 125.40 (Aryl- C_{para} and Aryl- C_{meta}), 110.33, 109.37 ($\text{CH}^{1,8}$ and $\text{CH}^{3,6}$), 39.11, 36.37 ($2 \times$ $\text{ThCH}_2\text{CMe}_3$), 36.05, 23.96 ($2 \times$ CMe_2), 35.97, 35.35 ($2 \times$ $\text{ThCH}_2\text{CMe}_3$), 35.13 (CMe_2), 34.90 (CMe_3), 31.43 (CMe_3), 29.44, 28.08 ($2 \times$ CHMe_2), 27.03, 25.77, 25.36, 24.33 ($4 \times$ CHMe_2).

[(XA₂)Th(CH₂SiMe₃)(CH₂CMe₃)] (5-Th; in Situ). A mixture of $[(\text{XA}_2)\text{Th}(\text{CH}_2\text{SiMe}_3)_2] \cdot 0.50(\text{SiMe}_3)_2$ (**1-Th**-0.50(SiMe_3)₂) (0.020 g, 0.017 mmol) and 2.2 equiv of $\text{LiCH}_2\text{CMe}_3$ (0.0030 g, 0.04 mmol) were taken up in toluene- d_8 to afford a colorless solution. Five minutes after mixing, ^1H NMR revealed new signals corresponding to an approximate 1:1:3:1 mixture of **5-Th**, **2-Th**, free $\text{LiCH}_2\text{SiMe}_3$, and remaining $\text{LiCH}_2\text{CMe}_3$, with concomitant loss of **1-Th**. ^1H NMR of **5-Th** (toluene- d_8 , 600.1 MHz, 298 K): δ 7.29, 7.21 (dd, $^3J_{\text{H,H}} = 7.7$ Hz; $^4J_{\text{H,H}} = 1.7$ Hz, $2 \times 2\text{H}$, Aryl-meta), 7.26 (t, $^3J_{\text{H,H}} = 7.7$ Hz, 2H , Aryl-para), 6.77, 6.04 (d, $^4J_{\text{H,H}} = 2$ Hz, $2 \times 2\text{H}$, $\text{CH}^{1,8}$ and $\text{CH}^{3,6}$), 3.83, 3.32 (broad sept, $^3J_{\text{H,H}} = 7$ Hz, $2 \times 2\text{H}$, CHMe_2), 1.70, 1.64 (s, $2 \times 3\text{H}$, CMe_2), 1.50, 1.32, 1.25, 1.08 (d, $^3J_{\text{H,H}} = 7$ Hz, $4 \times 6\text{H}$, CHMe_2), 1.19 (s, 18H , CMe_3), 0.74 (s, 9H , $\text{ThCH}_2\text{CMe}_3$), 0.21 (broad s, 2H , $\text{ThCH}_2\text{CMe}_3$), 0.05 (s, 9H , $\text{ThCH}_2\text{SiMe}_3$), -0.11 (broad s, 2H , $\text{ThCH}_2\text{SiMe}_3$). $^{13}\text{C}\{^1\text{H}\}$ NMR of **5-Th** (toluene- d_8 , 150 MHz, 298 K): δ 148.36, 147.86 ($2 \times$ Aryl- C_{ortho}), 148.23 ($\text{C}^{2,7}$), 145.92 ($\text{C}^{4,5}$), 142.0 ($\text{C}^{1,12}$), 135.66 (Aryl- C_{ipso}), 129.79 ($\text{C}^{10,13}$), 128.26 (Aryl- C_{para}), 125.55, 125.48 ($2 \times$ Aryl- C_{meta}), 110.49, 110.19 ($\text{CH}^{1,8}$ and $\text{CH}^{3,6}$), 37.44 ($\text{ThCH}_2\text{CMe}_3$), 35.54 ($\text{ThCH}_2\text{CMe}_3$), 35.26 (CMe_2), 35.12 (CMe_3), 33.87, 28.33 ($2 \times$ CMe_2), 31.63 (CMe_3), 29.43, 28.47 ($2 \times$ CHMe_2), 26.92, 25.91, 25.46, 24.77 ($4 \times$ CHMe_2), 3.48 ($\text{ThCH}_2\text{SiMe}_3$).

■ ASSOCIATED CONTENT

§ Supporting Information

Figures giving ^1H NMR spectra of **1** (variable temperature), **3** (variable temperature), **4**, **1-Th**, **2-Th**, and **5-Th** and CIF files giving crystallographic data for **1**, **2**, and **4**. This material is available free of charge via the Internet at <http://pubs.acs.org>.

■ AUTHOR INFORMATION

Corresponding Author

*Tel: 905-525-9140. Fax: 905-522-2509. E-mail: emslie@mcmaster.ca.

Notes

The authors declare no competing financial interest.

■ ACKNOWLEDGMENTS

D.J.H.E. thanks the NSERC of Canada for a Discovery Grant, and N.R.A. thanks the Government of Ontario for an Ontario Graduate Scholarship (OGS) and McMaster University for a Richard Fuller Memorial Scholarship.

■ REFERENCES

- (1) Burns, C. J.; Neu, M. P.; Boukhalfa, H.; Gutowski, K. E.; Bridges, N. J.; Rogers, R. D., Chapter 3.3: The Actinides. In *Comprehensive Coordination Chemistry II*; Parkin, G. F. R., Ed.; Elsevier: San Diego, CA, 2004; Vol. 3, p 189.
- (2) Fox, A. R.; Bart, S. C.; Meyer, K.; Cummins, C. C. *Nature* **2008**, 455, 341.
- (3) Cruz, C. A.; Emslie, D. J. H.; Harrington, L. E.; Britten, J. F.; Robertson, C. M. *Organometallics* **2007**, 26, 692.
- (4) (a) Fortier, S.; Melot, B. C.; Wu, G.; Hayton, T. W. *J. Am. Chem. Soc.* **2009**, 131, 15512. (b) Fortier, S.; Walensky, J. R.; Wu, G.; Hayton, T. W. *J. Am. Chem. Soc.* **2011**, 133, 11732.
- (5) Duhović, S.; Khan, S.; Diaconescu, P. L. *Chem. Commun.* **2010**, 46, 3390.
- (6) Kraft, S. J.; Fanwick, P. E.; Bart, S. C. *J. Am. Chem. Soc.* **2012**, 134, 6160.
- (7) Seaman, L. A.; Walensky, J. R.; Wu, G.; Hayton, T. W. *Inorg. Chem.* **2012**, DOI: 10.1021/ic300867m.
- (8) (a) Takats, J. Organactinide Complexes Containing Classical Ligands. In *Fundamental and Technological Aspects of Organo-f-Element Chemistry*; Marks, T. J., Fraga, I. L., Eds.; D. Reidel: Dordrecht, The Netherlands, 1985; NATO Science Series C, Vol. 155, p 159. (b) Marks, T. J.; Day, V. W. Actinide Hydrocarbyl and Hydride

Chemistry. In *Fundamental and Technological Aspects of Organo-f-Element Chemistry*; Marks, T. J., Fragalà, I. L., Eds.; D. Reidel: Dordrecht, The Netherlands, 1985; NATO Science Series C, Vol. 155, p 115. (c) Burns, C. J.; Clark, D. L.; Sattelberger, A. P., Actinides: Organometallic Chemistry. In *Encyclopedia of Inorganic Chemistry*; King, R. B., Lukehart, C. M., Eds.; Wiley: Chichester, England, 2005; Vol. 1, p 33.

(9) Only terminal alkyl complexes are included in Figure 1. Metalated ligand complexes or complexes of ylide, aryl, alkynyl, or π -allyl ligands are not included.

(10) Campello, M. P. C.; Calhorda, M. J.; Domingos, Â.; Galvão, A.; Leal, J. P.; de Matos, A. P.; Santos, I. J. *Organomet. Chem.* **1997**, 538, 223.

(11) (a) Silva, M.; Marques, N.; de Matos, A. P. *J. Organomet. Chem.* **1995**, 493, 129. (b) Domingos, Â.; Marques, N.; de Matos, A. P.; Santos, I.; Silva, M. *Organometallics* **1994**, 13, 654. (c) Matson, E. M.; Forrest, W. P.; Fanwick, P. E.; Bart, S. C. *J. Am. Chem. Soc.* **2011**, 133, 4948. (d) Matson, E. M.; Forrest, W. P.; Fanwick, P. E.; Bart, S. C. *Organometallics* **2012**, 31, 4467.

(12) Campello, M. P. C.; Domingos, Â.; Galvão, A.; de Matos, A. P.; Santos, I. J. *Organomet. Chem.* **1999**, 579, 5.

(13) Wedler, M.; Knösel, F.; Edelmann, F. T.; Behrens, U. *Chem. Ber.* **1992**, 125, 1313.

(14) Jantunen, K. C.; Batchelor, R. J.; Leznoff, D. B. *Organometallics* **2004**, 23, 2186.

(15) (a) Jantunen, K. C.; Haftbaradaran, F.; Katz, M. J.; Batchelor, R. J.; Schatte, G.; Leznoff, D. B. *Dalton Trans.* **2005**, 3083. (b) Hayes, C. E.; Leznoff, D. B. *Organometallics* **2010**, 29, 767. (c) Hayes, C. E.; Platel, R. H.; Schafer, L. L.; Leznoff, D. B. *Organometallics* **2012**, 31, 6732.

(16) Cruz, C. A.; Emslie, D. J. H.; Jenkins, H. A.; Britten, J. F. *Dalton Trans.* **2010**, 39, 6626.

(17) Cruz, C. A.; Emslie, D. J. H.; Robertson, C. M.; Harrington, L. E.; Jenkins, H. A.; Britten, J. F. *Organometallics* **2009**, 28, 1891.

(18) (a) Monreal, M. J.; Diaconescu, P. L. *Organometallics* **2008**, 27, 1702. (b) Duhović, S.; Monreal, M. J.; Diaconescu, P. L. *J. Organomet. Chem.* **2010**, 695, 2822.

(19) Cruz, C. A.; Emslie, D. J. H.; Harrington, L. E.; Britten, J. F. *Organometallics* **2008**, 27, 15.

(20) Korobkov, I.; Gambarotta, S.; Yap, G. P. A. *Angew. Chem., Int. Ed.* **2003**, 42, 814.

(21) Vidjayacoumar, B.; Ilango, S.; Ray, M. J.; Chu, T.; Kolpin, K. B.; Andreychuk, N. R.; Cruz, C. A.; Emslie, D. J. H.; Jenkins, H. A.; Britten, J. F. *Dalton Trans.* **2012**, 41, 8175.

(22) In **1-Th**, α -agostic interactions were confirmed by small $^1J_{^{13}\text{C},^1\text{H}}$ coupling constants for the ThCH_2 groups. The $\text{An}-\text{CH}_2-\text{SiMe}_3$ angles in **1-Th** were 126.8(3) and 127.6(3)°. In paramagnetic **1** and **2**, $^1J_{^{13}\text{C},^1\text{H}}$ coupling constants could not be measured; therefore, it is not possible to draw any definite conclusions from the expanded U-C-E (E = Si, C) angles.

(23) Shannon, R. D. *Acta Crystallogr.* **1976**, A32, 751.

(24) (a) Wetzel, D. M.; Brauman, J. I. *J. Am. Chem. Soc.* **1988**, 110, 8333. (b) Damrauer, R.; Kass, S. R.; Depuy, C. H. *Organometallics* **1988**, 7, 637.

(25) The thermodynamic driving force for conversion of **1** to **2** and **4** could alternatively be related to different levels of aggregation for the $\text{LiCH}_2\text{CMe}_3$ and MeLi reactants versus the $\text{LiCH}_2\text{SiMe}_3$ product in solution. However, this explanation seems unlikely, given that the reaction to form **2** was performed in an aromatic solvent while the reaction to form **4** was performed in THF, and the extent of alkyllithium aggregation in THF can be expected to be significantly less than that in benzene or toluene.

(26) Liu, B.; Liu, X. L.; Cui, D. M.; Liu, L. *Organometallics* **2009**, 28, 1453.

(27) Klimpel, M. G.; Eppinger, J.; Sirsch, P.; Scherer, W.; Anwander, R. *Organometallics* **2002**, 21, 4021.

(28) Mani, G.; Gabbai, F. P. *Angew. Chem., Int. Ed.* **2004**, 43, 2263.

(29) (a) Samsel, E. G.; Eisenberg, D. C. (Ethyl Corporation, USA). US Patent 5,276,220, 1994. (b) Kretschmer, W. P.; Bauer, T.; Hessen,

B.; Kempe, R. *Dalton Trans.* **2010**, 39, 6847. (c) Kretschmer, W. P.; Meetsma, A.; Hessen, B.; Schmalz, T.; Qayyum, S.; Kempe, R. *Chem. Eur. J.* **2006**, 12, 8969. (d) Hey, T. W.; Wass, D. F. *Organometallics* **2010**, 29, 3676.

(30) Ni Bhriain, N.; Brintzinger, H. H.; Ruchatz, D.; Fink, G. *Macromolecules* **2005**, 38, 2056.

(31) Wei, J.; Zhang, W.; Sita, L. R. *Angew. Chem., Int. Ed.* **2010**, 49, 1768.

(32) Lin, W. T.; Niu, H.; Chung, T. C. M.; Dong, J. Y. *J. Polym. Sci., Polym. Chem.* **2010**, 48, 3534.

(33) Arriola, D. J.; Carnahan, E. M.; Hustad, P. D.; Kuhlman, R. L.; Wenzel, T. T. *Science* **2006**, 312, 714.

(34) Pelletier, J. F.; Mortreux, A.; Olonde, X.; Bujadoux, K. *Angew. Chem., Int. Ed. Engl.* **1996**, 35, 1854.

(35) (a) Hartwig, J. F., *Organotransition Metal Chemistry: From Bonding to Catalysis*; University Science Books: Sausalito, CA, 2010. (b) Crabtree, R. H., *The Organometallic Chemistry of the Transition Metals*, 3rd ed.; Wiley: Toronto, 2001.

(36) (a) Schlenk, W.; Holtz, J. *Chem. Ber.* **1917**, 262. (b) Zieger, H.; Perri, C.; Bharucha, K. *Tetrahedron Lett.* **1987**, 28, 5989.

(37) Evans, W. J.; Traina, C. A.; Ziller, J. W. *J. Am. Chem. Soc.* **2009**, 131, 17473.

(38) Soria Alvarez, C.; Boss, S. R.; Burley, J. C.; Humphry, S. M.; Layfield, R. A.; Kowenicki, R. A.; McPartlin, M.; Rawson, J. M.; Wheatley, A. E. H.; Wood, P. T.; Wright, D. S. *Dalton Trans.* **2004**, 3481.

(39) Brinkmann, C.; García, F.; Morey, J. V.; McPartlin, M.; Singh, S.; Wheatley, A. E. H.; Wright, D. S. *Dalton Trans.* **2007**, 1570.

(40) Fernández-Cortabitarte, C.; García, F.; Morey, J. V.; McPartlin, M.; Singh, S.; Wheatley, A. E. H.; Wright, D. S. *Angew. Chem., Int. Ed.* **2007**, 46, 5425.

(41) Haywood, J.; Stokes, F. A.; Less, R. J.; McPartlin, M.; Wheatley, A. E. H.; Wright, D. S. *Chem. Commun.* **2011**, 47, 4120.

(42) Cruz, C. A.; Chu, T.; Emslie, D. J. H.; Jenkins, H. A.; Harrington, L. E.; Britten, J. F. *J. Organomet. Chem.* **2010**, 695, 2798.

(43) Kiplinger, J. L.; Morris, D. E.; Scott, B. L.; Burns, C. J. *Organometallics* **2002**, 21, 5978.

(44) Schrock, R. R.; Fellmann, J. D. *J. Am. Chem. Soc.* **1978**, 100, 3359.

(45) van der Sluis, P.; Spek, A. L. *Acta Crystallogr.* **1990**, A46, 194.